CODEN IEJMAT *Internet Electronic Journal of Molecular Design* **2006**, *5*, 530–541 ISSN 1538–6414
BioChem Press http://www.biochempress.com

Inter*net* Electronic Journal of Molecular Design

November 2006, Volume 5, Number 11, Pages 530–541

Editor: Ovidiu Ivanciuc

Special issue dedicated to Professor Lemont B. Kier on the occasion of the 75th birthday

Theoretical Studies on the Structural Change in the *N*–Protonated β–Octamethylporphyrin

Yuting Liao [1,2] and Siyu Ma [1]

[1] Department of Chemistry, Beijing Normal University, Beijing 100875, People's Republic of China
[2] Department of Applied Chemistry, East China Institute of Technology, Fuzhou 344000, People's Republic of China

Received: March 1, 2006; Revised: June 20, 2006; Accepted: July 1, 2006; Published: December 17, 2006

Citation of the article:
Y. Liao and S. Ma, Theoretical Studies on the Structural Change in the *N*–Protonated β–Octamethylporphyrin, *Internet Electron. J. Mol. Des.* **2006**, *5*, 530–541, http://www.biochempress.com.

Inter*net* Electronic Journal of Molecular Design

BioChem Press
http://www.biochempress.com

Theoretical Studies on the Structural Change in the *N*–Protonated β–Octamethylporphyrin

Yuting Liao [1,2] and Siyu Ma [1,*]

[1] Department of Chemistry, Beijing Normal University, Beijing 100875, People's Republic of China

[2] Department of Applied Chemistry, East China Institute of Technology, Fuzhou 344000, People's Republic of China

Received: March 1, 2006; Revised: June 20, 2006; Accepted: July 1, 2006; Published: December 17, 2006

Internet Electron. J. Mol. Des. **2006**, *5* (11), 530–541

Abstract

Motivation. The structural changes of four pyrrole–rings and various substituting groups of porphyrin derivatives have great influence on the selectivity to molecular aggregation in DNA helix; the aggregate can stabilize the DNA helix and disable telomerase. It not only can develop new anticancer drugs, but also can distinguish G–quadruplexes. Therefore, researchers are showing increasing interest in searching selective porphyrin compounds and understanding the structural change in acidic medium. In this paper, we report a theoretical calculation of β–octamethylporphyrin (β–$OMPH_2$) as well as its diacid (β–$OMPH_4^{2+}$) with an attempt to elucidate the changes of the configuration and property in the protonation process. The results calculated by B3LYP/6–1G* show that although β–$OMPH_2$ has various conformations, D_{2h}L configuration is the only stable equilibrium geometry. After protonation, the stable equilibrium configuration of β–$OMPH_4^{2+}$ presents D_{2d} symmetry. The configurational change is determined by a molecular intrinsic attribute and the intermolecular interaction is a secondary factor at least. The D_{4h} configuration of β–$OMPH_4^{2+}$ guessed by experimenters is a saddle point of multi–order, not a stable equilibrium configuration. In addition, a decrease in E_{2u} separation occurs concomitantly with an increase of degeneracy between a_{1u} and a_{2u}. These will lead to producing shift and strengthening absorbance of B and Q absorption bands.

Method. By means of B3LYP method combining Becke's three–parameter hybrid functional method with Lee–Yang–Parr's correlation functional (LYP) and Berny energy gradient method, the target molecules under reasonable symmetry restriction were optimized at 6–31G* basis set level. All of the stationary points were confirmed by vibrational analysis. In all calculations GAUSSIAN 98 program was used on a P4 computer.

Results. The change of the geometry between β–$OMPH_2$ and β–$OMPH_4^{2+}$ is obvious that leads to a series of property changes, especially, the change of FMO leads to a larger change of molecular absorption spectrum.

Conclusions. Although β–$OMPH_2$ has various conformations, D_{2h}L configuration is the only stable equilibrium geometry. After protonation, the stable equilibrium configuration of β–$OMPH_4^{2+}$ presents D_{2d} symmetry. The configurational change is determined by a molecular intrinsic attribute and the intermolecular interaction is a secondary factor at least. The D_{4h} configuration of β–$OMPH_4^{2+}$ guessed by experimenters is a saddle point of multi–order, not a stable equilibrium configuration. In the protonation process, along with the averaged bond lengths, the bond charge populations are also averaged generally. Although the changes are opposite with those of bond lengths in general, the exception exists. As expected, the energies of both the LUMOs and HOMOs of

Dedicated to Professor Lemont B. Kier on the occasion of the 75th birthday.

* Correspondence author; phone: 86–10–6220–8390; fax: 86–10–6220–2075; E–mail: siyuma50@163.com.

β–$OMPH_4^{2+}$ are lower than those in their unprotonated form. In addition, a decrease in E_{2u} separation occurs concomitantly with an increase of degeneracy between a_{1u} and a_{2u}. These will lead to producing shift and strengthening absorbance of B and Q absorption bands. After protonation, the vibrational Raman displacements of the C_α–C_β bonds are shifted to higher frequencies as the populations are increased, while those of the C_β–C_β bonds are shifted to lower frequencies as the populations are decreased; and the Raman displacements of the C_α–C_m bonds do not change in general, and those of the C_α–N bonds of various positions are shifted to higher or lower frequencies with the population changes. With the equivalence of the pyrrole rings, the IR spectrum of β–$OMPH_4^{2+}$ is simpler than that of β–$OMPH_2$ because of the higher symmetry of the former species.

Keywords. β–Octamethylporphyrin; *N*–protonated diacid; configurational change; B3LYP/6–31G* method.

Abbreviations and notations

β–$OMPH_2$, β–octamethylporphyrin	β–$OMPH_4^{2+}$, diacid of β–octamethylporphyrin
FMO, frontier molecular orbital	HOMO, highest occupied molecular orbital
LUMO, lowest unoccupied molecular orbital	$TPPH_2$, tetraphenylporphyrin
$TPPH_4^{2+}$, diacid of tetraphenylporphyrin	

1 INTRODUCTION

The structural changes of four pyrrole–rings and various substitutent groups of porphyrin derivatives have great influence on the selectivity to molecular aggregation in DNA helix [1]; the aggregate can stabilize the DNA helix and disable telomerase. It not only can develop new anticancer drugs, but also can distinguish G–quadruplexes. Therefore, researchers are showing increasing interest in searching selective porphyrin compounds and understanding the structural change in acidic medium. In the past several decades, a large number of theoretical researches on the porphyrin have been carried out. In the mid–90s, with the development of computer techniques and theoretical methods, revolutionary breakthrough on the structures has been found, and the theoretical results, which are consistent with experiments, have been obtained [2]. The study [3] shows that the structural changes of porphine in the protonation process are consistent with experiments [4] by using methods mentioned in this text. For the above–mentioned reasons, in this paper we report a theoretical calculation of β–octamethylporphyrin (β–$OMPH_2$) as well as its diacid (β–$OMPH_4^{2+}$) with an attempt to elucidate the effects of the substituted methyls, which are the typical repulsive electron groups, on the changes of the configuration and property in the protonation process.

2 COMPUTATIONAL METHODS

In order to investigate the relative change of the configuration in the protonation process, on the basis of other similar theoretical studies [3,5–10], we optimized the target large molecules by using B3LYP/6–31G* method [11–13], with the Berny gradient technique [14], under reasonable symmetry restriction. The B3LYP/6–31G* method provides an economical means for calculations of the structures and properties of porphyrin systems; and the calculation under symmetry restriction can aid us in studying the indivisible expression of normal modes with less CPU time [2]. Because of the D_{2h} symmetry of the porphine core, when a hydrogen atom in each β–substituted

methyls is in the porphine core plane, and others are over and under the plane respectively, the symmetry can be retained. Once the β–substituted methyls deviate from this angle, the symmetry of porphine skeleton can be reduced and the whole molecule symmetry would also be reduced. For *N*–protonated diacid, the free rotation of the β–substituted methyls cannot affect the D_{2d} symmetry of the porphine core and whole molecule, but in acid solution, because of the existence of rapid exchange of the inner hydrogens with solvent protons, the porphine core has a dynamically averaged D_{4h} symmetry [15,16]. If a hydrogen atom in each β–substituted methyls is in the porphine core plane, and others are over and under the plane respectively, the whole molecule also has D_{4h} symmetry. In all calculations GAUSSIAN 98 program [17] was used on a P4 computer.

3 RESULTS AND DISCUSSION

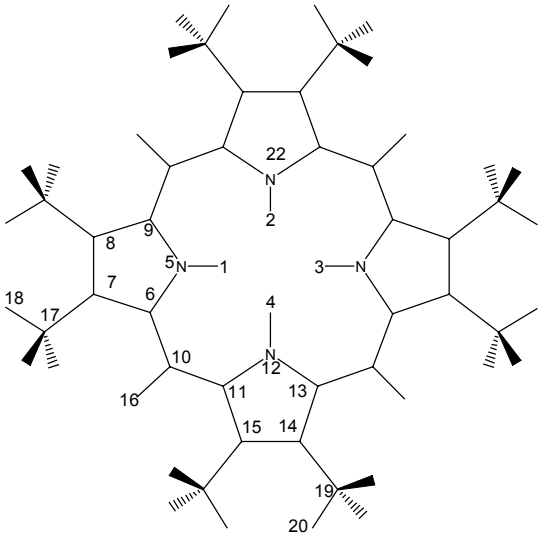

Figure 1. Atomic numbering of the system.

Table 1. The Bond Lengths (nm) of β–$OMPH_2$ and β–$OMPH_4^{2+}$

Bond Length	$OMPH_2$ (D_{2h}L)	$OMPH_4^{2+}$ (D_{2d})	$OMPH_4^{2+}$ (D_{4h}L)	Bond Length	$OMPH_2$ (D_{2h}L)	$OMPH_4^{2+}$ (D_{2d})	$OMPH_4^{2+}$ (D_{4h}L)
N_5–H_1	0.1015	0.1014	0.0994	C_{15}–C_{14}	0.1364	0.1392	0.1389
C_6–N_5	0.1370	0.1394	0.1379	C_{11}–C_{10}	0.1400	0.1395	0.13402
C_7–C_6	0.1444	0.1435	0.1446	H_{16}–C_{10}	0.1086	0.1084	0.1085
C_8–C_7	0.1381	0.1392	0.1389	C_{19}–C_{14}	0.1499	0.1496	0.1498
N_{12}–C_{11}	0.1362	0.1394	0.1379	C_{17}–C_7	0.1500	0.1496	0.1498
C_{13}–C_{14}	0.1470	0.1435	0.1446	H_{20}–C_{19}	0.1094	0.1092	0.1091
C_{10}–C_6	0.1370	0.1392	0.1402	H_{18}–C_{17}	0.1093	0.1092	0.1091

3.1 The Structures of β–$OMPH_2$ and β–$OMPH_4^{2+}$

The main axis (C_2) of the D_{2h} configuration of β–$OMPH_2$ is a line crossing molecular center and perpendicular to the porphine core plane, the two C_2 axes perpendicular to the main axis are two lines crossing the H_1–H_3 and N_{12}–N_{22}, respectively; and σ_h is the porphine core plane. In each β–

methyls, when one hydrogen atom is in the porphine core plane, and other two are over and under the plane respectively, then the two D_{2h} configurations are found: D_{2h}H and D_{2h}L. All geometric parameters are given in Tables 1–3 (for the numbering of atoms, see Figure 1). The configurational diagrams are shown in Figure 2.

Table 2. The Bond Angles (°) of β–$OMPH_2$ and β–$OMPH_4^{2+}$

Bond Angle	$OMPH_2$ (D_{2h}L)	$OMPH_4^{2+}$ (D_{2d})	$OMPH_4^{2+}$ (D_{4h}L)	Bond Angle	$OMPH_2$ (D_{2h}L)	$OMPH_4^{2+}$ (D_{2d})	$OMPH_4^{2+}$ (D_{4h}L)
$\angle C_9N_5H_1$	124.6	119.6	123.7	$\angle C_{13}C_{14}C_{15}$	107.7	107.9	108.0
$\angle C_6C_{10}C_{11}$	127.7	127.9	130.3	$\angle N_5C_6C_{10}$	124.3	125.0	125.9
$\angle C_6N_5C_9$	110.6	108.7	112.3	$\angle N_{12}C_{11}C_{10}$	124.4	125.0	125.9
$\angle C_8C_9N_5$	107.0	107.8	105.6	$\angle H_{16}C_{10}C_6$	116.0	116.5	114.8
$\angle C_7C_8C_9$	107.5	107.7	108.0	$\angle H_{16}C_{10}C_{11}$	116.0	116.5	114.8
$\angle C_{11}N_{12}C_{13}$	105.2	108.7	112.3	$\angle H_{18}C_{17}C_7$	111.3	110.8	111.5
$\angle N_{12}C_{13}C_{14}$	111.5	107.8	105.6	$\angle H_{20}C_{19}C_{14}$	111.3	110.8	111.5

Table 3. The Dihedral Angles (°) of β–$OMPH_4^{2+}$ (D_{2d})

Dihedral Angle	$OMPH_4^{2+}$ (D_{2d})	Dihedral Angle	$OMPH_4^{2+}$ (D_{2d})
$\angle C_6C_7C_8C_9$	0.0	$\angle H_{16}C_{10}C_6C_7$	8.7
$\angle C_7C_8C_9N_5$	–2.8	$\angle H_{18}C_{17}C_7C_8$	22.8
$\angle C_8C_9N_5H_1$	147.3	$\angle H_{18}C_{17}C_7C_6$	–160.0
$\angle C_6C_{10}C_{11}N_{12}$	9.5	$\angle C_{19}C_{14}C_{13}N_{12}$	174.8
$\angle C_7C_6C_{10}C_{11}$	–171.3		

When the β–methyls in β–$OMPH_2$ (D_{2h}H) are rotated by 180.0°, this configuration is changed into D_{2h}L. In addition, the distance between the H in σ_h plane and the neighboring *m*–H in D_{2h}H configuration is about 0.205 nm, while the distance between two neighboring Hs in σ_h plane in D_{2h}L configuration is about 0.208 nm; so it is clear that because the steric repulsion between the neighboring atoms is small, D_{2h}L configuration is lower in energy (the difference is 17.5 kJ/mol) than that of D_{2h}H configuration. Normal–mode analysis of D_{2h}H yields several imaginary frequencies, which shows that D_{2h}H is not stable; while the normal–mode analysis of D_{2h}L confirms it to be the correct equilibrium structure (no imaginary frequency exists).

Obviously, considering the different orientations of hydrogen atoms in the plane, also there are two C_{2h} configurations: C_{2h}A and C_{2h}B (the configurational diagrams are shown in Figure 3). And the normal–mode analysis of C_{2h}A and C_{2h}B yields several imaginary frequencies, which shows that they are also not stable. In addition, considering of free rotation of the β–methyls, usually σ_h will disappear, and the C_{2v}, C_2, D_2 configurations of β–$OMPH_2$ may exist. But the calculated results show that these optimized configurations are similar to the D_{2h}L configuration. In a word, the D_{2h}L configuration (the geometric parameters are given in Tables 1–2) is the only stable equilibrium structure.

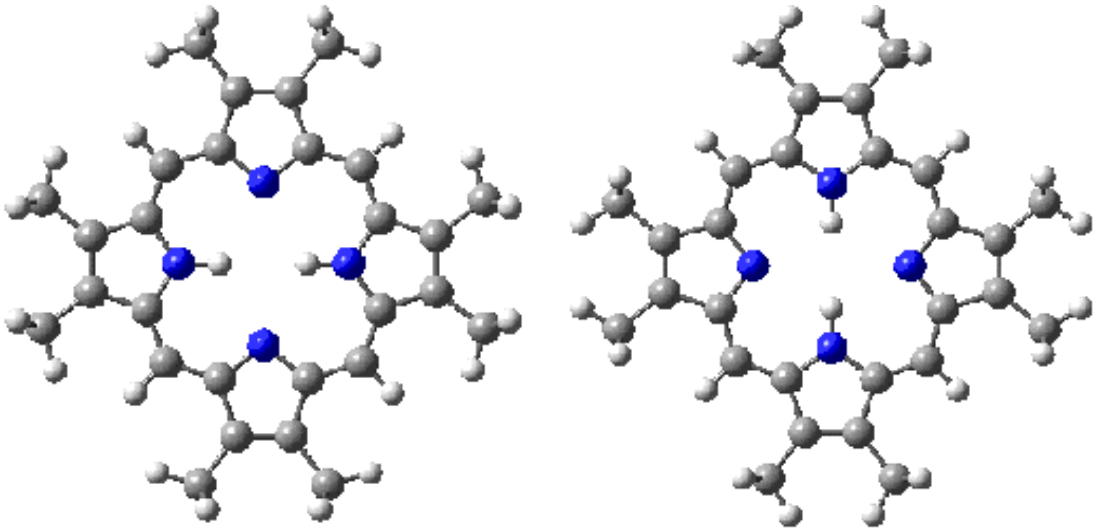

D_{2h}H D_{2h}L

Figure 2. Optimized configuration of β–$OMPH_2$ (D_{2h}H and D_{2h}L).

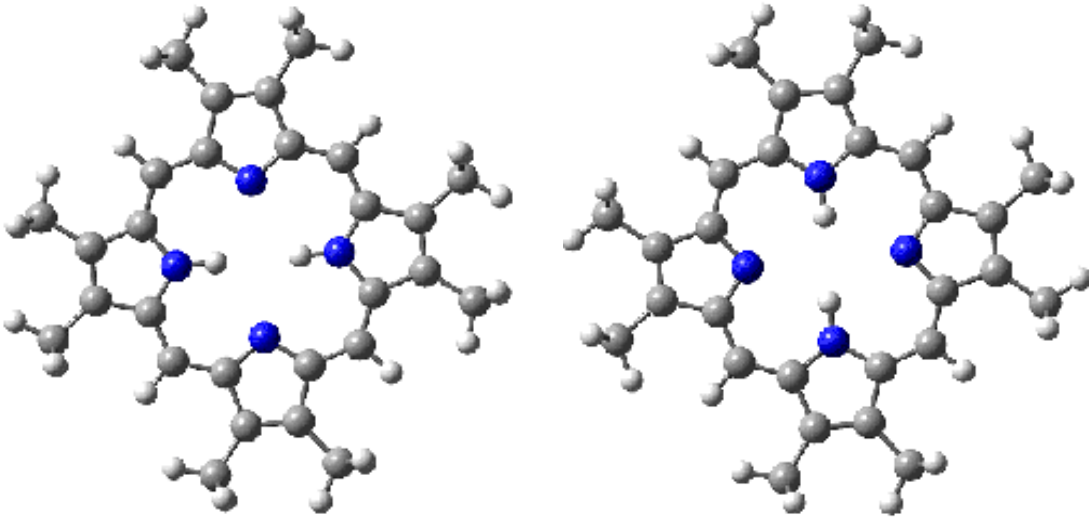

C_{2h}A C_{2h}B

Figure 3. Optimized configuration of β–$OMPH_2$ (C_{2h} A and C_{2h} B).

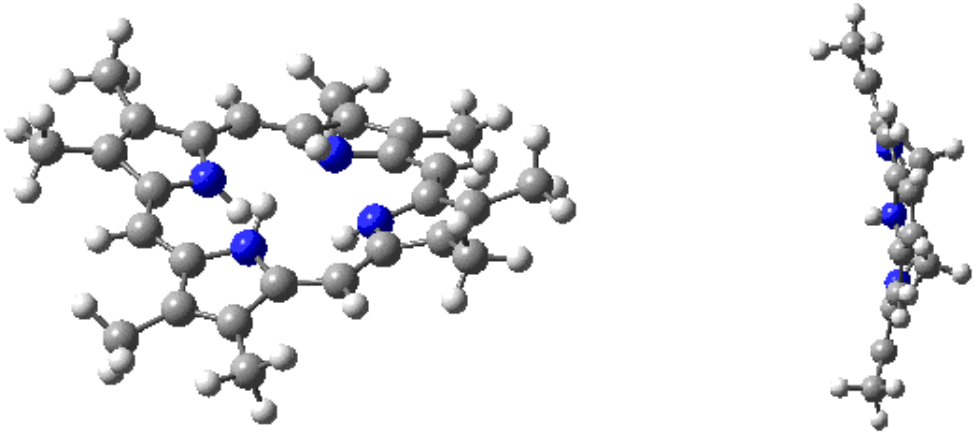

Figure 4. Optimized configuration and its side view of β–$OMPH_4^{2+}$ (D_{2d}).

After the protonation, because of the steric effect of the inner neighboring hydrogens, in D_{2d} configuration, the pyrrole rings flip up and down in alternate directions with the rotation angle being 9.5°, and the dihedral angles of β–methyls and pyrrole ring are 32.7° ($\angle H_{20}C_{19}C_{14}C_{13}$=147.3). The main axis is unchanged; the two C_2 axes perpendicular to the main axis are diagonals crossing opposite C_m atoms; the two σ_d planes dividing the angle between the two C_2 axes equally are the planes crossing the main axis and the inner opposite H–H line. The geometric parameters are given in Tables 1–3, and the configurational diagrams with D_{2d} are presented in Figure 4.

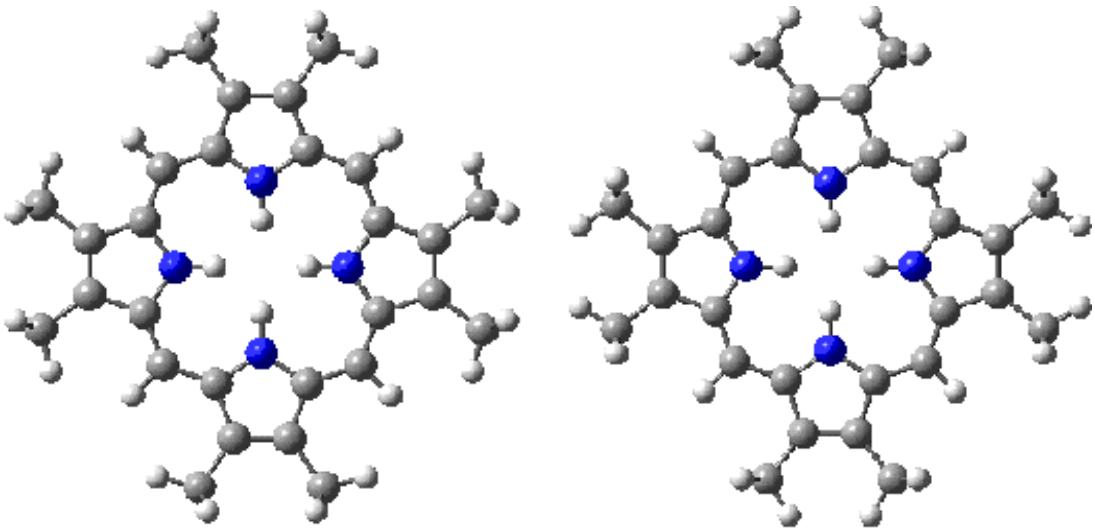

D_{4h}H D_{4h}L

Figure 5. Optimized configuration of *β*–$OMPH_4^{2+}$ (D_{4h}H and D_{4h}L).

It is interesting to note that the side views of the configurations show that the molecular skeleton is shaped like a bowl from D_{2h} to D_{2d}. These can provide important information concerning molecular aggregation undoubtedly. Generally, the deviation of pyrrole rings from the porphine core plane is unfavorable to molecular aggregation; but β–$OMPH_4^{2+}$ has a center of symmetry with S_4 axis, and its shape is favorable to orderly aggregation. If there is a rapid exchange between the inner hydrogens and solvent protons, the exchange vibration of the bowl–shaped molecular aggregate is also favorable.

Analyzing their configuration parameters, especially, the changes of D_{2d} relative to D_{2h}L, because of the existence of S_4, C_α–N, C_α–C_β, C_β–C_β and C_α–C_m bonds are averaged. Notably, it changes the parameters of pyrrole rings, especially, on the rings having N_{12} and N_{22}. C_α–N bonds (C_6–N_5 and C_{11}–N_{12}) are increased by 2.4 pm and 2.8 pm, and C_β–C_β bonds (C_8–C_7 and C_{15}–C_{14}) are increased by 1.1 pm and 3.2 pm, while C_α–C_β bonds (C_7–C_6 and C_{14}–C_{13}) are reduced by 0.9 pm and 3.5 pm, respectively. C_α–C_m bonds (C_{10}–C_6 and C_{11}–C_{10}) are also increased by 2.2 pm and 0.5 pm. In addition, the bond lengths of C–H in methyls are changed slightly after protonation.

It is obvious that there are two D_{4h} configurations, which are consistent with two D_{2h}

configurations respectively. D_{4h}L configuration is lower in energy than that of D_{4h}H configuration (see Figure 5), and the energy difference is 3.4 kJ/mol, so we only discuss D_{4h}L configuration. Normal–mode analysis of D_{4h}L yields four imaginary frequencies (see Figure 6), which is consistent with those calculated results of protonated porphine [5]. So it is expected that β–$OMPH_4^{2+}$ also have three kinds of saddle points of multi–order (two C_{2h} configurations and one C_{4v} configuration), as the same as PH_4^{2+} (D_{4h}). In addition, the energy of the dynamic D_{4h}L configuration of β–$OMPH_4^{2+}$ (for the geometric parameters, see Tables 1–3) is increased by 98.8 kJ/mol over the D_{2d} configuration. Finally, when the S_4 changes into C_4, because of the planar restriction of the porphine core, the parameter changes of pyrrole rings are notable. N–H bonds are reduced by 2.0 pm, and C_α–N bonds are reduced by 1.5 pm while C_α–C_β bonds are increased by 1.1 pm, respectively. The diagonal of porphine ring is increased by 4.3 pm, and the corresponding bond angles are increased and reduced by 0.1~4.1°.

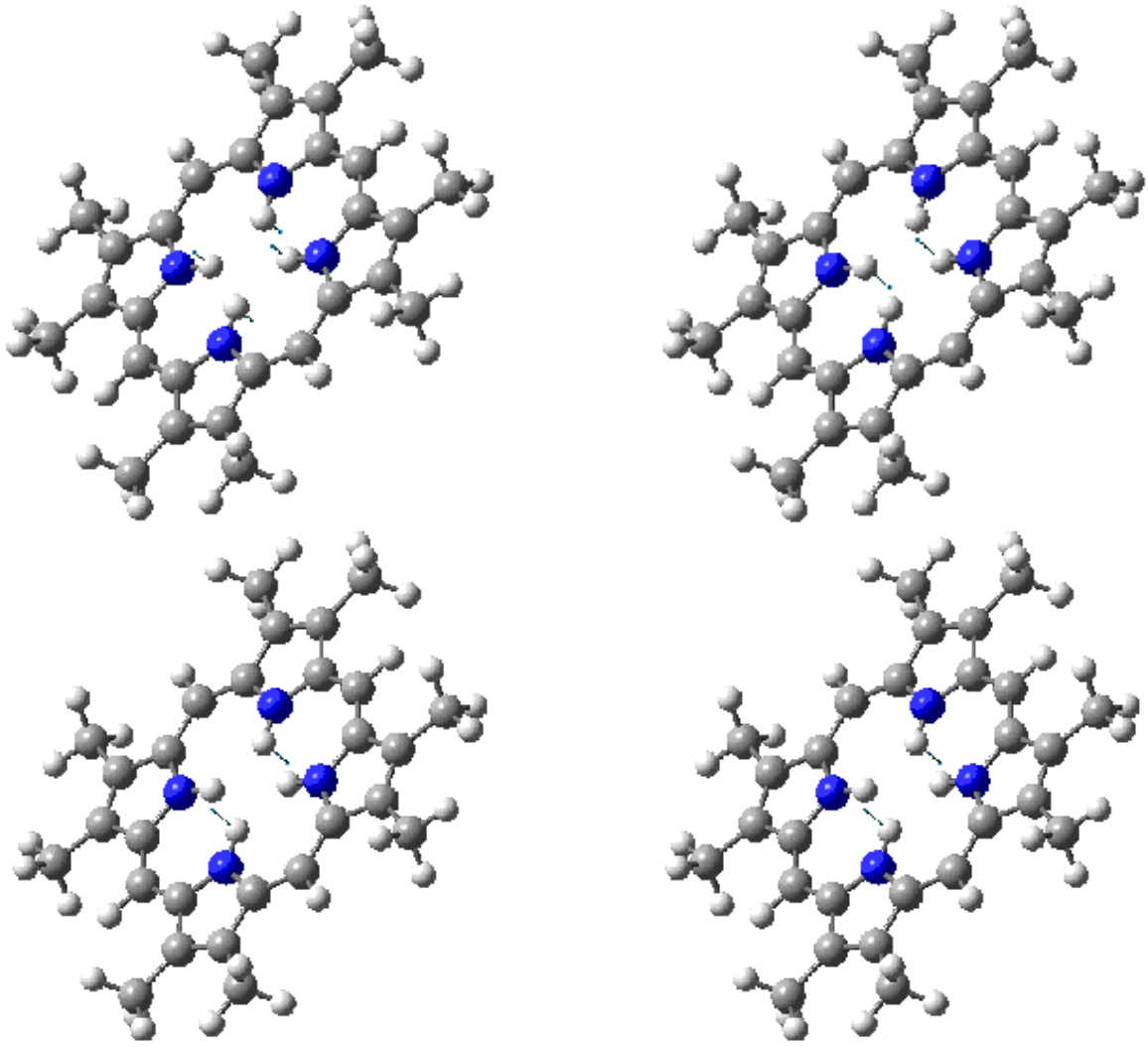

Figure 6. The imaginary frequency modes of β–$OMPH_4^{2+}$ (D_{4h}L).

3.2 The Bond Charge Populations of β–$OMPH_2$ and β–$OMPH_4^{2+}$

Seen from the data of GAUSSIAN 98 (see Table 4), it is clear that the bond charge populations are also averaged in protonation process. Although the changes are opposite with those of bond lengths in general, the exception exists, for example, C_6–N_5 of C_α–N is reduced by 0.0272 *e*, C_8–C_7 and C_{15}–C_{14} of C_β–C_β are reduced by 0.0140 *e* and 0.0357 *e*, respectively; but N_{12}–C_{11} of C_α–N is increased by 0.0240*e*, which is same with the increase of bond lengths. The population changes of D_{4h} relative to D_{2d} are opposite with the changes of bond lengths, for example, the bond charge populations of C_α–N and C_β–C_β are increased by 0.0148 *e* and 0.0038 *e*, respectively while that of C_α–C_β are reduced by 0.0038 *e*. These provide useful insights of changes of the aggregate selectivity.

Table 4. The bond charge populations (e) of β–$OMPH_2$ and β–$OMPH_4^{2+}$

bond	$OMPH_2$ (D_{2h}L)	$OMPH_4^{2+}$ (D_{2d})	$OMPH_4^{2+}$ (D_{4h}L)	bond	$OMPH_2$ (D_{2h}L)	$OMPH_4^{2+}$ (D_{2d})	$OMPH_4^{2+}$ (D_{4h}L)
N_5–H_1	0.2941	0.2912	0.3043	C_{15}–C_6	0.4533	0.4523	0.4519
C_6–N_5	0.3743	0.3471	0.3619	C_{11}–C_{10}	0.4500	0.4523	0.4519
C_7–C_6	0.4165	0.4190	0.4152	H_{16}–C_{10}	0.3831	0.3755	0.3757
C_8–C_7	0.5078	0.4938	0.4974	C_{17}–C_7	0.3474	0.3418	0.3415
N_{12}–C_{11}	0.3231	0.3471	0.3619	C_{19}–C_{14}	0.3477	0.3418	0.3415
C_{13}–C_{14}	0.3785	0.4190	0.4152	H_{18}–C_{17}	0.3659	0.3627	0.3685
C_{15}–C_{14}	0.5295	0.4938	0.4974	H_{20}–C_{19}	0.3656	0.3627	0.3685

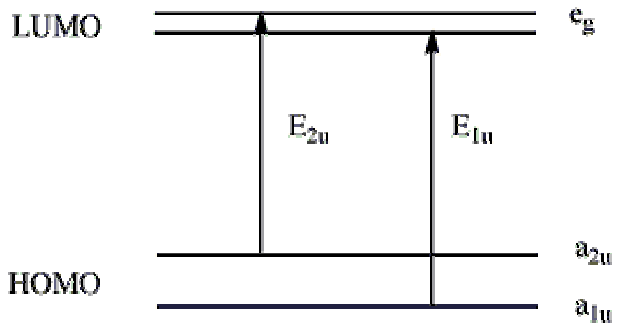

Figure 7. Sketch diagram of frontier orbital energy levels of porphyrins.

3.3 The Effects of *N*–Protonated Structure Change on Molecular Spectra

Gouterman's four–orbital model of porphyrin derivatives can be used as a tool for explaining their absorption spectra. The model [18] shows that in an ideal D_{4h} point group, the HOMO has two near energy levels (a_{1u} and a_{2u}), and the LUMO has two degenerate e_g energy levels. They factitiously define two transitions of single excitation (see Figure 7): E_{1u} ($a_{1u}\rightarrow e_g$) and E_{2u} ($a_{2u}\rightarrow e_g$). The two transition moments having the same direction interact and produce the B absorption band (near 420 nm), and those having opposite direction interact and produce the Q absorption band (near 514 nm). The frontier molecular orbital (FMO) levels of the various configurations of β–$OMPH_2$ and β–$OMPH_4^{2+}$ are given in Table 5.

Table 5. The FMO Levels (eV) of β–$OMPH_2$ and β–$OMPH_4^{2+}$

FMO	orbital number	$OMPH_2$ (D_{2h}L)	$OMPH_4^{2+}$(D_{2d})	$OMPH_4^{2+}$(D_{4h}L)
LUMO	115	B_{2g} –1.89	E –8.88	E_g –8.96
	114	B_{3g} –1.90	E –8.88	E_g –8.96
HOMO	113	B_{1u} –4.82	B_2 –11.77	A_{2u} –11.86
	112	A_u –4.88	B_1 –11.78	A_{1u} –11.95

We can see from Table 5 that the two LUMOs are degenerate while the two HOMOs are closely spaced, which is in accordance with Gouterman's model. In addition, the transition energy level differences also change after protonation (for data see Table 6), mainly the E_{2u} is reduced. As expected, the quantitative analysis of the changes in the protonation process further reveals that the energies of both the LUMOs and HOMOs of β–$OMPH_4^{2+}$ are lower than those in their unprotonated form. In addition, a decrease in E_{2u} separation occurs concomitantly with an increase of degeneracy between a_{1u} and a_{2u} (see Table 6). According to Gouterman's theory, these will lead to producing shift and strengthening absorbance of B and Q absorption bands.

Table 6. The Separations of Transition Energy Level (eV) of β–$OMPH_2$ and β–$OMPH_4^{2+}$

E_u	$OMPH_2$ (D_{2h}L)	$OMPH_4^{2+}$ (D_{2d})	$OMPH_4^{2+}$ (D_{4h}L)
E_{2u}	2.93	2.88	2.90
E_{1u}	2.98	2.89	2.99

Meanwhile, one can infer the changes of molecular Raman displacement from the changes of the bond charge population on the porphine skeleton in the protonation process. After the protonation, the population changes on the C–C and C–N bonds are notable (see the analysis in Section 3.2) because the bond charge population on the neighboring pyrroles is averaged. Since the population change determines the change in the intervals of vibrational energy levels and further determines their Raman displacements, one can predict that the vibrational Raman displacements of the C_α–C_β bonds are shifted to higher frequencies as the populations are increased while those of the C_β–C_β bonds are shifted to lower frequencies as the populations are decreased; and the Raman displacements of the C_α–C_m bonds do not change in general and those of the C_α–N bonds of various positions are shifted to higher or lower frequencies with the population changes.

Finally, the infrared spectra of β–octamethylporphyrin also change in the protonation process. After protonation, with the equivalence of the pyrrole rings, the IR spectrum of β–$OMPH_4^{2+}$ is simpler than that of β–$OMPH_2$, due to the higher symmetry of the former species.

3.4 The Change in the Orientation of Pyrrole Rings

We found that in the cofigurational optimization of *β*–$OMPH_4^{2+}$ when the pyrrole rings deviate from the porphine core plane, the energy is favorable. In fact, the energy of D_{2d} configuration of β-$OMPH_4^{2+}$ is reduced by 98.8 kJ/mol in comparison with the D_{4h}L configuration. Why there is this large reduction in energy as the molecule deviates from a stable conjugate system? In studying the

crystal structure of tetraphenylporphyrin and its diacid ($TPPH_2$ and $TPPH_4^{2+}$), Stone *et al*. [19] have proposed that there are two main causes for the non–planar configuration of the gas phase $TPPH_4^{2+}$: one is the steric hindrance of the inner neighboring hydrogens, and the other is their electrostatic interaction. But Scheidt [20] considered that the cause is intermolecular interaction and is not an intrinsic attribute. Although these conclusions are made in studying the crystal structure of tetraphenylporphyrin, we can infer from them that in β–octamethylporphyrin, the phenomenon of pyrroles deviating from the porphine core plane results from intermolecular or intramolecular interactions. The calculations of this paper are done for the gas phase and isolated molecular condition. The preceding analyses show that the configurational change is determined by a molecular intrinsic attribute and the intermolecular interaction is a secondary factor, at least.

Table 7 gives the data of distances between inner hydrogens in β–$OMPH_4^{2+}$. Because the effective Van der Waals diameter of hydrogen is 0.22~0.24 nm [21], the Van der Waals interaction between the opposite hydrogens (H_1–H_3, H_2–H_4) in a planar porphine skeleton (D_{4h}L) does not exist but a stronger interaction between the neighboring hydrogens (H_1–H_2, H_1–H_4, H_3–H_2, H_3–H_4) exists.

Table 7. The distances (nm) of inner hydrogens of β–$OMPH_4^{2+}$

β–$OMPH_4^{2+}$	H_1–H_3	H_2–H_4	H_1–H_2	H_3–H_2	H_1–H_4	H_3–H_4
(D_{4h}L)	0.2360	0.2360	0.1660	0.1660	0.1660	0.1660
(D_{2d})	0.2685	0.2685	0.2301	0.2301	0.2301	0.2301

In addition, H_1, H_2, H_3 and H_4 of β–$OMPH_4^{2+}$ all have net positive charges (0.3216e (D_{2d}) and 0.2794e (D_{4h}L), respectively). As the neighboring hydrogens in a planar molecule are near, the electrostatic interaction is notable. These results are consistent with Stone's guess.

4 CONCLUSIONS

Although β–$OMPH_2$ has various conformations, D_{2h}L configuration is the only stable equilibrium geometry. After protonation, the stable equilibrium configuration of β–$OMPH_4^{2+}$ presents D_{2d} symmetry. The configurational change is determined by a molecular intrinsic attribute and the intermolecular interaction is a secondary factor at least. The D_{4h} configuration of β–$OMPH_4^{2+}$ guessed by experimenters is a saddle point of multi–order, not a stable equilibrium configuration. In protonation process, along with the averaged bond lengths, the bond charge populations are also averaged generally. Although the changes are opposite with those of bond lengths in general, the exception exists. As expected, the energies of both the LUMOs and HOMOs of β–$OMPH_4^{2+}$ are lower than those in their unprotonated form. In addition, a decrease in E_{2u} separation occurs concomitantly with an increase of degeneracy between a_{1u} and a_{2u}. These will

lead to producing shift and strengthening absorbance of B and Q absorption bands. After protonation, the vibrational Raman displacements of the C_α–C_β bonds are shifted to higher frequencies as the populations are increased, while those of the C_β–C_β bonds are shifted to lower frequencies as the populations are decreased; and the Raman displacements of the C_α–C_m bonds do not change in general, and those of the C_α–N bonds of various positions are shifted to higher or lower frequencies with the population changes. With the equivalence of the pyrrole rings, the IR spectrum of β–$OMPH_4^{2+}$ is simpler than that of β–$OMPH_2$ because of the higher symmetry of the former species.

5 REFERENCES

[1] S. Borman, Quadruplex DNA: Anticancer Knot? *Chem Engng News*. **1998**, *5*, 42–53.
[2] A. Ghosh, J. Almlöf, Structure and Stability of *cis*–Porphyrin, *J. Phys. Chem*. **1995**, *99*, 1073–1075
[3] S. Y. Ma, Y. T. Liao, The Effect of Methods and Basis Sets of the Symmetric Structure of Porphine, *J. Beijing Normal University* (*Natural Science*) **2003**, *39*, 107–114.
[4] B. M. L. Chen, A. Tulinsky, Redetermination of the Structure of Porphine, *J. Am. Chem. Soc*. **1972**, *94*, 4144–4151.
[5] Y. T. Liao, Y.L. Zhang, S. Y. Ma, A Theoretical Study on the Substituent Effect of Porphine Symmetry, *J. Beijing Normal University* (*Natural Science*) **2005**, *41*, 608–612.
[6] Y. T. Liao, M.H. Wang, S. Y. Ma, A Theoretical Study on the Structural Change in the *N*–Protonated β–Octaethylporphyrin, *J. Beijing Normal University* (*Natural Science*) **2004**, *40*, 647–654.
[7] X. F. Huang, S. Y. Ma, R. Z. Liu, Theoretical Studies on the Structural Change of the *N*–Protonated Tetraphenylporphyrin (II) The Effects of the Substituting Groups Fluorines, *Chem. Res. Chinese Universities* **2002**, *23*(8), 1562–1566.
[8] S. Y. Ma, J. Wang, Studies on the Structural Change of the *N*–Protonated Tetrapyridylporphine II.The Effects of the Substituting Group *meso*–(p–Methylpyridyl), *Acta Chimica Sinica* **2001**, *59*(2), 195–200.
[9] S. Y. Ma, Z. H. Li, Theoretical Studies on the Structural Change of the *N*–Protonated Tetrapyridylporphine, *Acta Chimica Sinica* **2000**, *58*, 588–593.
[10] S. Y. Ma, Q. J. Yue, Z. H. Li, Theoretical Studies on the Structural Change in the *N*–Protonated tetraphenylporphyrin, *Science in China*, *Ser. B* **2000**, *30*, 103–109.
[11] D. Becke, Density–Functional Thermochemistry III: The Role of Exact Exchange, *J. Chem. Phys*. **1993**, *98*, 5648–5652.
[12] C. Lee, W. Yang, R. G. Parr, Development of the Colle–Salvetti Correlation–energy Formula into a Functional of the Electron Density, *Phys. Rev. B* **1998**, *37*, 785–789.
[13] B. Miehlich, A. Savin, H. Stoll, H. Preuss, Results Obtained with the Correlation Energy Density Functionals of Becke and Lee, Yang and Parr, *Chem. Phys. Lett*. **1989**, *157*, 200–206.
[14] H. B. Schlegel, New Gradient Method for Molecular Geometric Optimization, *J. Comput. Chem*. **1982**, *3*, 214–221.
[15] S. F. Mason, The Infrared Spectra of *N*–Heteroaromatic Systems, Part I. The Porphyrins, *J. Chem. Soc*. **1958**, 976–983.
[16] G. L. Closs, J. J. Katz, F. C. Pennington, M. R. Thomas, H. H. Strain, Nuclear Magnetic Resonance Spectra and Molecular Association of Chlorophylls A and B, Methyl Chlorophyllides, Pheophtins, and Methyl Pheophorbides, *J. Am. Chem. Soc*. **1963**, 85, 3809–3821.
[17] M. J. Frisch, G. W. Trucks, H. B. Schlegel, G. E. Scuseria, M. A. Robb, J. R. Cheeseman, V. G. Zakrzewski, J. A. Montgomery, Jr., R. E. Stratmann, J. C. Burant, S. Dapprich, J. M. Millam, A. D. Daniels, K. N. Kudin, M. C. Strain, O. Farkas, J. Tomasi, V. Barone, M. Cossi, R. Cammi, B. Mennucci, C. Pomelli, C. Adamo, S. Clifford, J. Ochterski, G. A. Petersson, P. Y. Ayala, Q. Cui, K. Morokuma, D. K. Malick, A. D. Rabuck, K. Raghavachari, J.

B. Foresman, J. Cioslowski, J. V. Ortiz, A. G. Baboul, B. B. Stefanov, G. Liu, A. Liashenko, P. Piskorz, I. Komaromi, R. Gomperts, R. L. Martin, D. J. Fox, T. Keith, M. A. Al–Laham, C. Y. Peng, A. Nanayakkara, M. Challacombe, P. M. W. Gill, B. Johnson, W. Chen, M. W. Wong, J. L. Andres, C. Gonzalez, M. Head–Gordon, E. S. Replogle, and J. A. Pople, GAUSSIAN 98 (Revision A.9), Gaussian Inc., Pittsburgh, PA, 1998.

[18] M. Gouterman, Four–orbital Model for Porphyrin Derivatives, *J. Mol. Spectrosc*. **1961**, *6*, 138–163.

[19] A. Stone, E. B. Fleischer, The Molecular and Crystal Structure of Porphyrin Diacids, *J. Am. Chem. Soc*. **1968**, *90*, 2735–2748.

[20] W. R. Scheidt, Y. J. Lee, *Structure and Bonding* **1987**, *64*, 17–45.

[21] A. I. Kitaigorodskii, Organic Chemical Crystallography, Consultants Bureau, New York, **1961**, pp. 7.

Biographies

Yuting Liao was a graduate student of physical chemistry at Beijing Normal University in 2000–2003. Now she is an assistant professor of quantum chemistry at the East China Institute of Technology in Fuzhou. She is engaged in teaching and research of computational chemistry.

Siyu Ma is a professor of physical chemistry at Beijing Normal University in Beijing. He is engaged in teaching and research of theoretical chemistry and computational chemistry. In recent years, his main research interests are relationship between molecular structure and property, chemical reaction mechanism and chemical reaction dynamics. He published more than 60 scientific papers.